





(17) NRL MK 401

SECURITY CLASSIFICATION OF THIS PAGE (When Data Entered)

9 REPORT DOCUMENTATION PAGE		READ INSTRUCTIONS BEFORE COMPLETING FORM
1. REPORT NUMBER NRL Memorandum Report 4618	2. GOVT ACCESSION NO. ADA 205709	3. RECIPIENT'S CATALOG NUMBER
4. TITLE (and Subtitle) PLASMA CONDITIONS REQUIRED FOR ATTAINMENT OF MAXIMUM GAIN IN RESONANTLY PHOTO-PUMPED Al XII AND Ne IX	5. TYPE OF REPORT & PERIOD COVERED Interim report on a continuing NRL problem.	
	6. PERFORMING ORG. REPORT NUMBER	
7. AUTHOR(s) J. P. Apruzese*, J. Davis, and K. G. Whitney	8. CONTRACT OR GRANT NUMBER(s)	
9. PERFORMING ORGANIZATION NAME AND ADDRESS Naval Research Laboratory Washington, DC 20375	10. PROGRAM ELEMENT PROJECT, TASK AREA & WORK UNIT NUMBERS 62704H; 47-0858-0-1	
11. CONTROLLING OFFICE NAME AND ADDRESS Defense Nuclear Agency Washington, DC 20305	12. REPORT DATE October 9, 1981	
	13. NUMBER OF PAGES 24	
14. MONITORING AGENCY NAME & ADDRESS (if different from Controlling Office)  10 25	15. SECURITY CLASS. (of this report) UNCLASSIFIED	
	15a. DECLASSIFICATION/DOWNGRADING SCHEDULE	
16. DISTRIBUTION STATEMENT (of this Report)  Approved for public release; distribution unlimited.		
17. DISTRIBUTION STATEMENT (of the abstract entered in Block 20, if different from Report)  T99QAXL (10) AD 4		
18. SUPPLEMENTARY NOTES *Present address: Science Applications, Inc., McLean, VA 22102 This research was sponsored by the Defense Nuclear Agency under Subtask T99QAXLA014, work unit 37, and work unit title, "Advanced Concepts Theory Program."		
19. KEY WORDS (Continue on reverse side if necessary and identify by block number) Plasma mixture Radiative pumping X-ray lasing Plasma diagnostics		
20. ABSTRACT (Continue on reverse side if necessary and identify by block number) We present a detailed analysis of the plasma conditions required to optimize gain in two proposed x-ray lasing schemes using resonant photo-pumping. In one proposed configuration, the Si XIII line $1s^2-1s2p^1P$ at 6.650 Å pumps Al XII $1s^2-1s3p^1P$ at 6.635 Å, inverting the Al XII $n = 3$ and $n = 2$ levels which are separated by 44 Å. A similar approach which utilizes the Na X $1s^2-1s2p^1P$ line at 11.00 Å to pump the Ne IX $1s^2-1s4p^1P$ line at 11.001 Å would invert the $n = 3$ and $n = 2$ levels of Ne IX, separated (Continues)		

DD FORM 1473 1 JAN 73

EDITION OF 1 NOV 65 IS OBSOLETE  
S/N 0102-014-6601

SECURITY CLASSIFICATION OF THIS PAGE (When Data Entered)

251950

## 20. ABSTRACT (Continued)

by 82 Å. Conditions in the pumped neon and aluminum plasmas, and in the pumping silicon plasma, are calculated using a multistage, multilevel atomic model with multi-frequency radiation transport. For modeling the pumping sodium line we have inferred the intensity from a spectrum of a neon filled, laser-imploded glass microballoon containing sodium impurities obtained at Rochester. It is found that peak gain of about  $100 \text{ cm}^{-1}$  occurs at ion densities of  $10^{20} \text{ cm}^{-3}$  and  $4 \times 10^{20} \text{ cm}^{-3}$  in the pumped neon and aluminum plasmas, respectively. At higher ion densities the inversions are rapidly collisionally quenched. Temperatures required to maximize gain in the pumped plasmas are found to be 50 eV and 100 eV, for neon and aluminum, respectively. Plasmas of lower temperature do not contain enough of the active ion species, whereas at higher temperatures the photon pumping of the upper levels results in excessive ionization from these levels to the hydrogen-like species. Finally, since the pumping silicon and pumped aluminum lines are slightly off resonance, we have investigated the effect of streaming the plasmas toward each other at various velocities to offset some or all of the wavelength difference. It is found that a streaming velocity of  $6.8 \times 10^7 \text{ cm sec}^{-1}$ —fully offsetting the wavelength difference—will approximately triple the achieved gain compared to the zero velocity case. Lesser increases in gain occur with partial velocity offsets.

CONTENTS

I. INTRODUCTION ..... 1

II. DESCRIPTION OF MODEL AND CALCULATIONS ..... 2

III. RESULTS OF GAIN CALCULATIONS ..... 6

IV. FURTHER REMARKS AND CONCLUSIONS ..... 13

V. ACKNOWLEDGMENT ..... 14

VI. REFERENCES ..... 15

Accession For	
NTIS GRA&I	<input checked="" type="checkbox"/>
DTIC TAB	<input type="checkbox"/>
Unannounced	<input type="checkbox"/>
Justification	
By _____	
Distribution/	
Availability Codes	
Dist	Avail and/or
	Special
A	

## PLASMA CONDITIONS REQUIRED FOR ATTAINMENT OF MAXIMUM GAIN IN RESONANTLY PHOTO-PUMPED Al XII AND Ne IX

### I. Introduction

It has been suggested<sup>1-4</sup> that population inversions in plasmas may be efficiently pumped by opacity broadened lines from different ionization stages of the same element or from different elements in a two component plasma. Experimental evidence<sup>5,6</sup> has been presented for inversions of the  $n = 4$  and  $n = 3$  levels in Mg XII and Mg XI, which were pumped by resonant Ly $\alpha$  and  $1s^2-1s2p^1P$  radiation in C VI and C V. The abovementioned lasing transitions in Mg lie at  $\sim 130$  and  $156$  A for Mg XII and Mg XI, respectively. In this paper we present a detailed analysis of the plasma conditions which would be needed to optimally implement two promising lasing schemes utilizing resonant photoexcitation with considerably shorter lasing wavelengths (82 A and 44 A). The radiation field--critical in a photoexcitation process--is modeled in detail. The pumped and pumping transitions--as well as other key optically thick lines--are calculated on a frequency grid allowing for accurate modeling of broadening processes and frequency-dependent absorption. Previous efforts at modeling short-wavelength resonantly photo-excited lasing processes have employed assumed linewidths<sup>1</sup>, line profiles arising from uniform source functions<sup>2</sup>, assumed power densities<sup>3,5</sup>, or probability-of-escape approximations<sup>4</sup>. In another study<sup>7</sup>, the pumped plasma was modeled with a fine frequency grid but the pumping spectrum was assumed to be a filtered Planckian. In section II our atomic model is described along with the methodology for its employment for calculations for both the pumped and pumping plasmas. In section III the equilibrium results are presented for optimum plasma densities, temperatures, and relative velocities and the relevant physical processes controlling these effects are analyzed. Finally, we summarize the work and present our basic conclusions in section IV.

## II. Description of Model and Calculations

### A. Basic Details of Models

The photon pumping schemes to be analyzed are the following. Scheme 1 would employ the Si XIII  $1s^2-1s2p^1P$  resonance line at  $6.650 \text{ \AA}$  to pump the Al XII  $1s^2-1s3p^1P$  resonance line at  $6.635 \text{ \AA}$ , creating an inversion of the  $n = 3$  and  $n = 2$  levels of Al XII. Scheme 2 utilizes the Na X  $1s^2-1s2p^1P$  line at  $11.00 \text{ \AA}$  to pump the Ne IX  $1s^2-1s4p^1P$  line at  $11.001 \text{ \AA}$ , creating an inversion primarily in the  $n = 3$  and  $n = 2$  levels of Ne IX. Scheme 1 results in stimulated emission at  $44 \text{ \AA}$  and scheme 2 at  $82 \text{ \AA}$ . Ionic state and level densities as well as the radiation field are computed for Al using the model described in ref. 7. For Si, a precisely analogous model to Al--the same level structure and transitions--is employed. The Ne atomic model is described in ref. 8. This model possesses an extra degree of sophistication in that self-consistent Stark profiles<sup>9</sup> are used for the line opacity rather than the Voigt profiles employed for Al and Si. For Na, no atomic model is employed. Rather, the profile of the pumping line at  $11.00 \text{ \AA}$  is utilized as it was experimentally measured from glass impurities in a laser implosion experiment at the University of Rochester<sup>10</sup>. The multifrequency measured profile is modified within the pumped neon plasma by absorption and re-emission in the Ne line and this phenomenology is computed in detail using the flux profile of the Na line as an input condition on the Ne plasma. Further details are given below in subsection C. Results given below are calculated for collisional-radiative equilibrium (CRE).

### B. Pumped Plasma Calculation

As previously pointed out<sup>6</sup>, radiation trapping effects in the pumped plasma can generally be minimized or eliminated by making the transverse dimensions of the plasma small. We have followed this approach in modeling the pumped plasma--the radiation field is calculated in a planar plasma of infinite area with thickness small enough to insure an optically thin regime over a broad angular range of specific intensities. Our objectives--given an optically thin lasing medium--are to determine a range of temperatures, densities, and, for scheme 1, streaming velocities that will optimize gain and to determine some of the tradeoffs involved. We have previously discussed trapping effects in the pumped plasma in refs. 4 and 7.

The pumped plasma is assumed to be bathed symmetrically in the pumping radiation which is calculated (for Si) or measured (for Na). The penetration of the pumping radiation into the pumped plasma is calculated in a straightforward manner. At the outer boundaries of the pumped plasma the inward specific intensity along each ray at each frequency  $I_{\nu}^{-}$  is taken to be that emitted from the pumping plasma which is also assumed to be planar. The radiative transfer equation is then solved in the pumped plasma with this particular boundary condition for  $I_{\nu}^{-}$  applied at each of the chosen rays at the outer boundaries of the pumped plasma. The calculation in the pumped plasma then proceeds by iteration until steady state conditions are obtained. Since fully coupled radiative transport and rate equations are solved in this model, the steady state obtained is a self-consistent collisional radiative equilibrium. The quantity of primary interest here--the gain coefficient of the lasing transition--is obtained as a linear function of the computed densities of the upper and lower states. Finally, the temperature, density and (for Al) velocity of the pumped plasma was varied in order to obtain the functional dependence of the gain coefficient on these quantities. We make no attempt to calculate the depletion of excited states by lasing, and thus are computing only the linear amplifier behavior.

### C. Treatment of the Pumping Plasma

Our principal objective is to determine the effect of varying conditions in the pumped plasma on the achieved gain. Therefore, we selected only one set of pumping conditions for each of the Si and Na plasmas. Since the  $1s^2-1s2p^1P$  Si XIII and  $1s^2-1s3p^1P$  Al XII lines are off resonance by 0.015 Å, the profile of the  $1s^2-1s2p^1P$  line must be wide enough to produce significant intensity at 0.015 Å (i.e. 13 Doppler widths at 400eV) from line center. Thus, for a stationary plasma the line must be opacity broadened<sup>2</sup>. If the resonance line is very thick at line center, the Lorentz wings will still exceed optical depth unity many Doppler widths from line center, guaranteeing a wide profile. Such conditions can be obtained in a moderate energy Si plasma of 1.5 mm width, temperature 400eV, and ion density  $8 \times 10^{19} \text{cm}^{-3}$ . Plasmas similar to this have been realized in the laboratory<sup>11</sup>. Most importantly, the CRE calculation for this plasma indicates that, depending on position, 62-82% of the ions are in the active (helium-like) stage. Furthermore, the optical depth of the pumping resonance line  $1s^2-1s2p^1P$  is  $\sim 500$ , which produces a very wide profile, as shown in Fig. 1. In addition to the calculated emission profile the

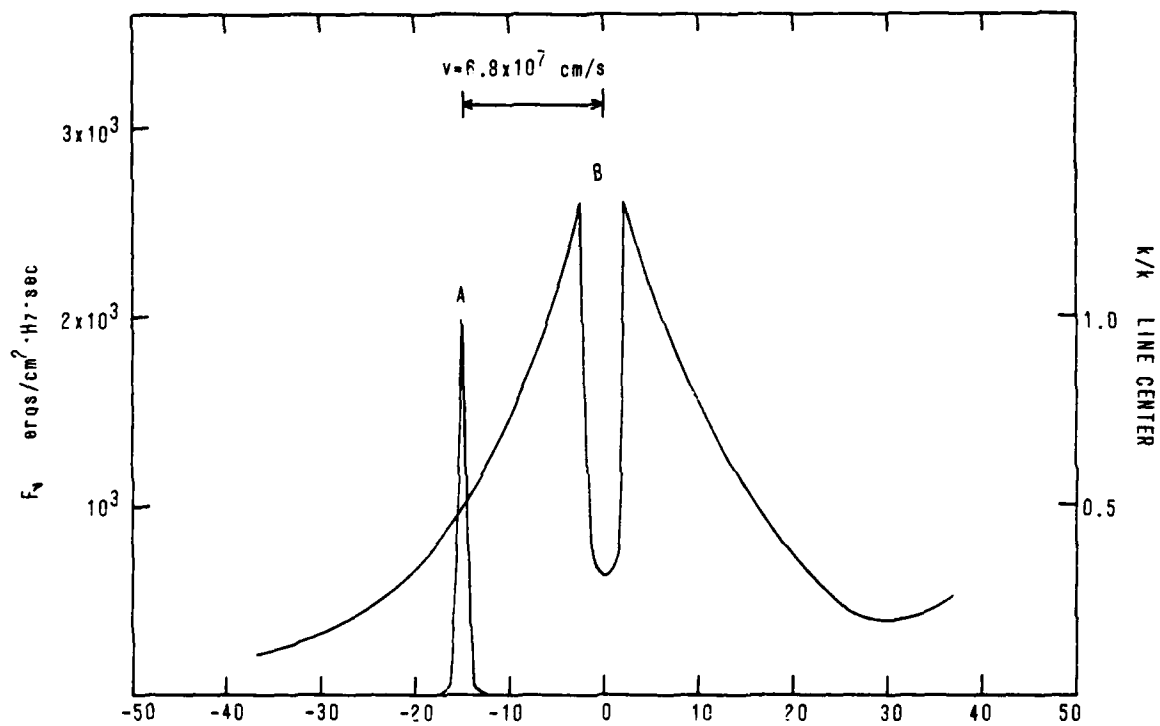


Fig. 1 — The line profile of the Si pumping line (B) calculated to arise from the indicated plasma conditions is shown on the same wavelength scale as the intrinsic absorption profile of the pumped Al line (A). The left vertical scale applies to the flux of the emitted Si line; the right vertical scale applies to the absorption coefficient of the Al line.

intrinsic absorption profile for the  $1s^2-1s3p^1P$  Al XII line is shown for typical conditions in the aluminum plasma. In this case, the Si resonance line is sufficiently broadened by opacity to overcome the resonance defect. Therefore, under the reasonable assumption that these equilibrium Si plasma conditions be achieved the Si/Al lasing scheme will be viable at least in this sense that the resonance defect can be overcome.

To obtain a radiation source to pump Ne, we have analyzed the spectrum of a laser-imploded neon filled glass microballoon obtained at Rochester<sup>10</sup>. One of the strongest lines appearing in this spectrum is that of the Na X  $1s^2-1s2p^1P$  line--which arose from sodium impurities in the glass. Since we have been able to reproduce the observed spectrum with a first-principles non-LTE calculation of the line and continuum intensities<sup>8</sup>, the theoretical calculation which matches the observed spectrum also yields the absolute intensities of the lines--(flux in  $\text{ergs}/\text{cm}^2\text{-sec-Hz}$ ) at the outer surface of the pellet. Knowing the absolute intensities of the Ne lines, one may infer the Na line intensity profile from its measured intensity relative to the Ne lines. Its value at the central peak is  $6.6 \times 10^3 \text{ ergs}/\text{cm}^2\text{-sec-Hz}$ . It is this intensity profile which we use as our pump source in the Na/Ne calculations discussed in the next section.

The frequency profile is the one appearing in the published spectrum<sup>10</sup>, where experimental sources of broadening are relatively small. In any event deconvoluting any experimental broadening would result in a sharper central peak, which, since the lines are perfectly resonant, would give a better pump source. In the next section it is shown that this experimentally observed Na X  $1s^2-1s2p^1P$  line intensity profile is sufficient to pump a substantial inversion in the Ne X  $n = 2$  and  $n = 3$  levels. This finding is significant in light of the fact that this radiation was merely a consequence of sodium impurities in the glass, i.e. no effort was made to increase its intensity in the experiment. We note that only the radiation of the Na resonance line was used to pump Ne, whereas the pumping effects of all the calculated Si radiation-pumping plus other lines plus continuum, were included in the Al calculation.

### III. Results of Gain Calculations

#### A. Density Dependence

A principal question related to the time varying conditions in the pumped plasma is: at what density is gain maximized? As has been often pointed out<sup>3,4,6,12</sup>, there exists for each lasing scheme contemplated a density above which no inversion is possible, due to the tendency of collisional processes to bring the state densities into LTE. At much lower densities one also expects that the gain coefficient will be reduced purely because there are fewer lasing ions in a given linear distance. It is evident that some density must exist at which the gain in steady state will be a maximum. This behavior is shown in Figs. 2 and 3, where the results of detailed calculations for various pumped plasma densities are presented for Si/Al and Na/Ne, respectively. In each case the gain for the strongest of the 2-3 lines (the 2p-3d) is plotted against the pumped plasma's density. For Ne, the assumption of statistical equilibrium for the  $n = 3$  singlet sublevels is enforced, whereas, for the Si/Al calculation, results are presented with this assumption both enforced and relaxed. The chosen temperatures approximately correspond to maximum values for gain, this point is discussed further in the next section. Note that substantial peak gains - of  $10^2 \text{ cm}^{-1}$  or more - are obtained for both schemes. For the Si/Al calculations, zero relative velocity between the two components was assumed. The assumption of statistical equilibrium leads to an overestimate of gain at low densities; however, for densities near the predicted peak gain, around  $4 \times 10^{20} \text{ cm}^{-3}$ , the overestimate is very slight. This effect is due to the increasing validity of the statistical equilibrium assumption at higher densities as collisional processes dominate the populating of the sublevels.

For Al, peak gain occurs at an ion (electron) density of  $4 \times 10^{20}$  ( $4.2 \times 10^{21}$ )  $\text{cm}^{-3}$ , for Ne the corresponding figures are  $10^{20}$  ( $8.1 \times 10^{20}$ )  $\text{cm}^{-3}$ . For hydrogenic lasing schemes, Bhagavatula<sup>3,6</sup> has presented reduced variable equations which demonstrate that the dependence of electron density at peak gain on  $Z$  is  $Z^7$ . We note with interest that the  $Z$ -dependence of electron density at peak gain implied by the above numbers for our helium-like schemes is fairly similar,  $Z^{6.3}$ .

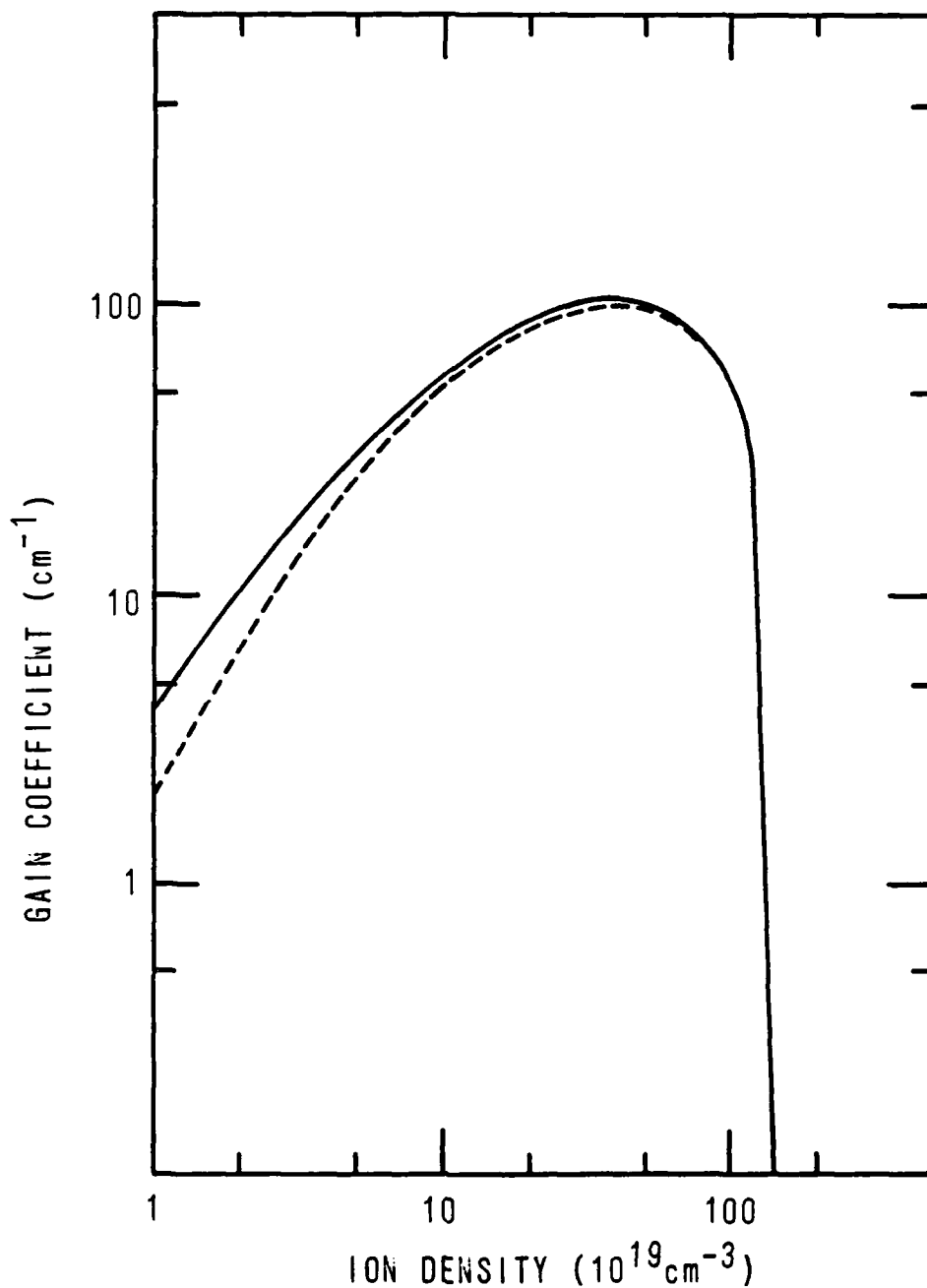


Fig. 2 — Line center gain coefficient in the Al XII  $2p^1P-3d^1D$  line is plotted vs. Al plasma ion density, with an assumed pumped plasma temperature of 100 eV. Dual results for the assumption of collisional equilibrium (solid line) between the  $3p-3d$  states and for a general, rate-by-rate treatment of these states are displayed. Characteristics of the pumping Si plasma are discussed in the text.

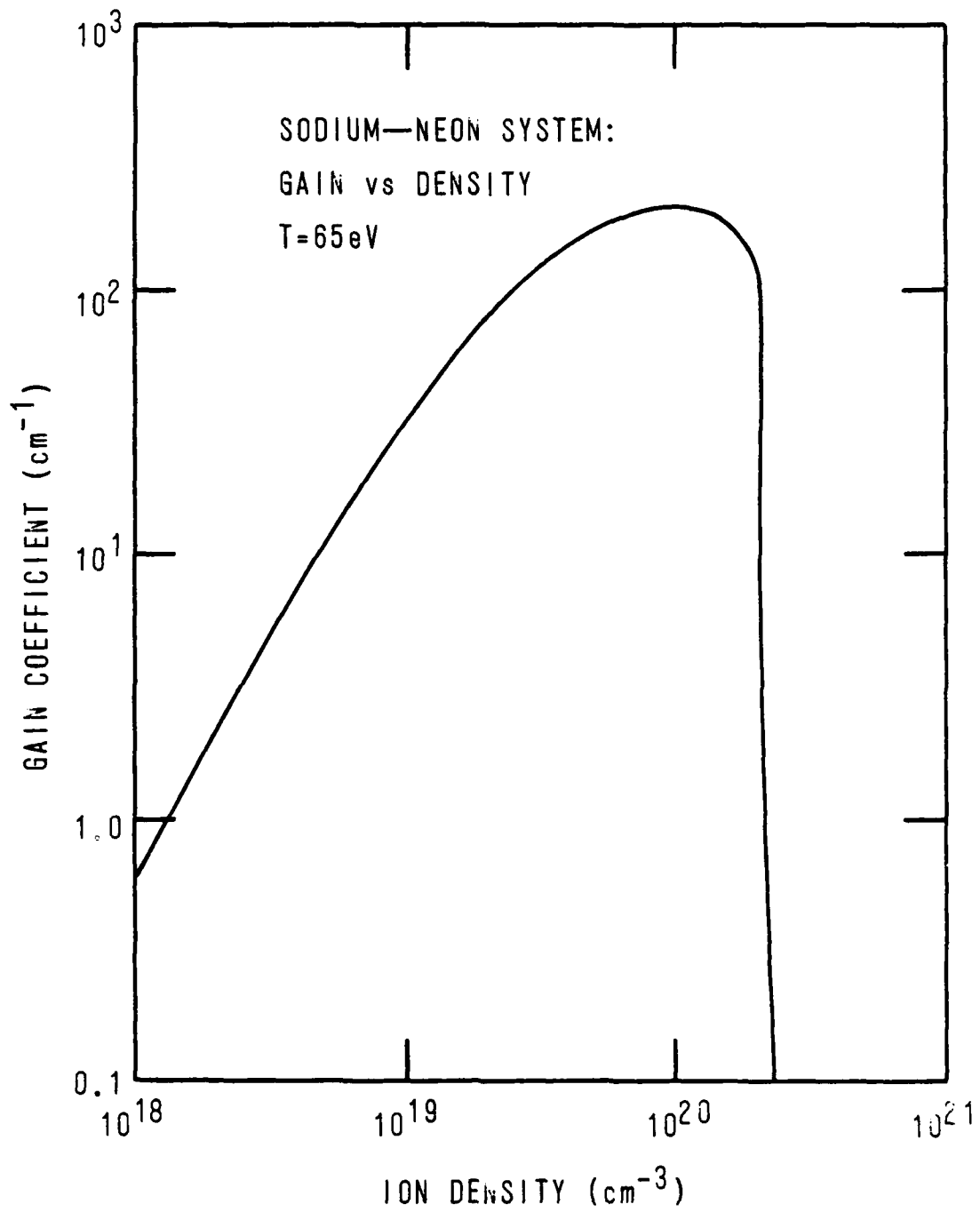


Fig. 3 — Line center gain coefficient in the Ne IX  $2p^1P-3d^1D$  line is plotted vs. Ne plasma ion density, for an assumed pumped plasma temperature of 65 eV.

## B. Temperature Dependence

In Figs. 4 and 5 results for gain vs. temperature are plotted for the Si/Al and Na/Ne systems for fixed ion densities of  $5 \times 10^{19} \text{ cm}^{-3}$  and  $10^{20} \text{ cm}^{-3}$ , respectively. The gain dependence on temperature is similar to that on density in that a maximum is exhibited with a sharp falloff on one side caused by the variation of the active ion species' populations with temperature. Note however, that the temperature of maximum gain is much lower than one would expect from coronal model calculations of the ionic species abundances. Such calculations<sup>13</sup> reveal that helium-like ion concentrations peak at 120eV and 330eV for Ne and Al, respectively. The present calculations predict corresponding peak gains at 50eV and 100eV. These lower pumped plasma temperatures are necessitated by the radiative pumping to the  $n = 4$  and  $n = 3$  bound levels in the two schemes which greatly facilitates collisional ionization. Hence peak lasing ion abundance is forced to much lower temperatures where fewer electrons are capable of ionization from these bound states. At still lower temperatures a sharp gain and abundance falloff occurs as the plasma assumes a more normal configuration when the "extra" ionization becomes small. In these two lasing systems, the strength of the pumping decisively affects the temperature at which the pumped plasma must be prepared for maximum gain to occur. Such effects have been noted elsewhere<sup>6,7</sup> in somewhat different contexts.

## C. Velocity Dependence

For the Na/Ne system, the pumped and pumping lines are within resonance to 1 part in  $10^5$ , and thus there is no question as to the adequacy of the wavelength coincidence. For Si/Al, however, the wavelength difference of  $0.015 \text{ \AA}$  amounts to 13 Doppler widths at 400eV. For a photon traveling at normal incidence to the pumped plasma, this resonance defect could be made up if the two plasmas stream toward each other at  $6.8 \times 10^7 \text{ cm sec}^{-1}$ . But given the wide opacity broadened pumping line profile (Fig. 1) the functional dependence of gain on plasma streaming velocity must be calculated; this result is presented in Fig. 6. In these calculations, the frequencies of the radiation incident on the pumped plasma were shifted angle-by-angle to reflect the streaming velocities indicated. Even though there is a substantial self-reversal at the center of the pumping line, peak gain does indeed occur for the matched streaming velocity of  $6.8 \times 10^7$

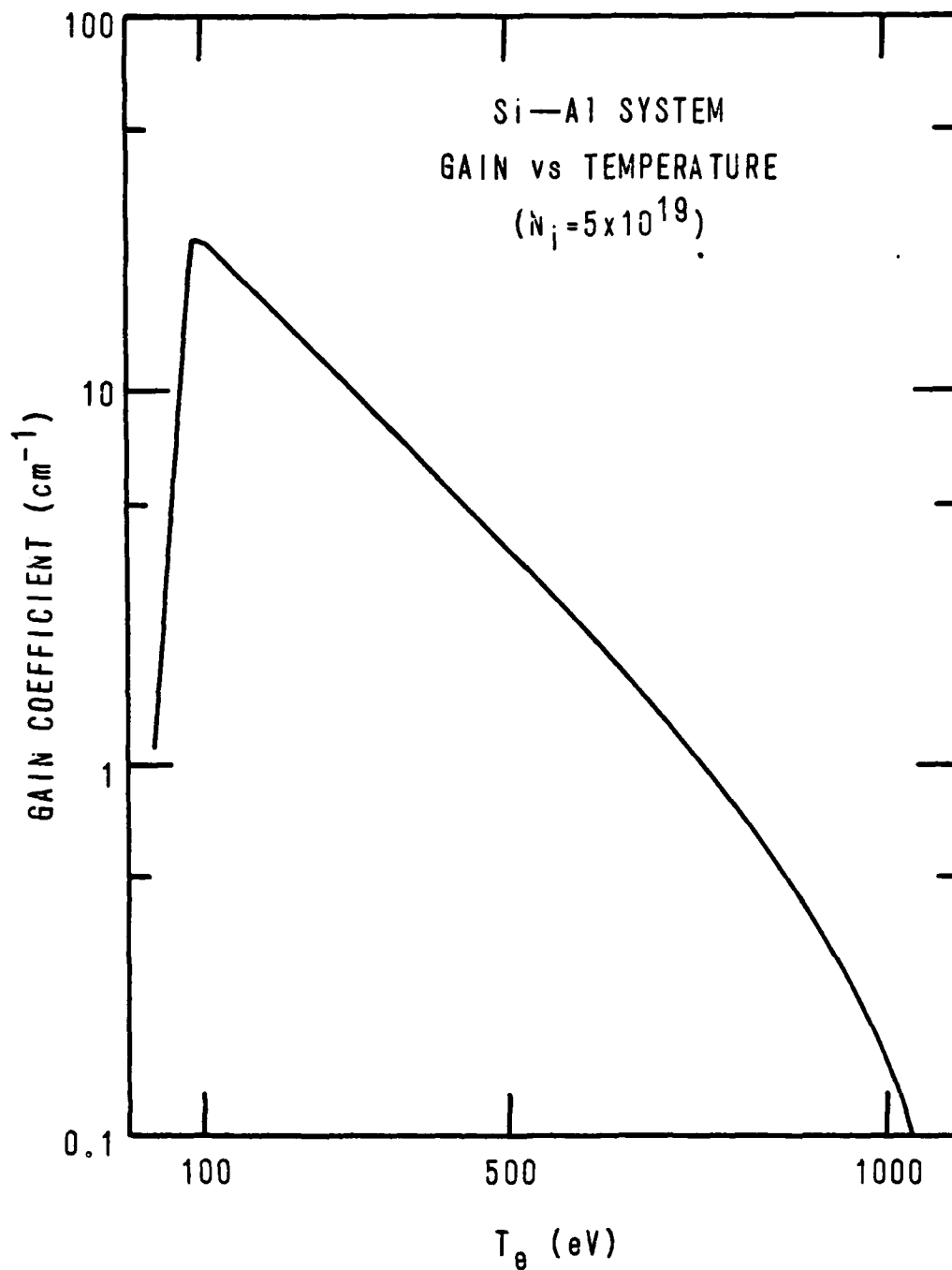


Fig. 4 — Line center gain coefficient in the Al XII  $2p^1P-3d^1D$  line is plotted vs. Al plasma temperature for a fixed Al ion density of  $5 \times 10^{19} \text{ cm}^{-3}$ .

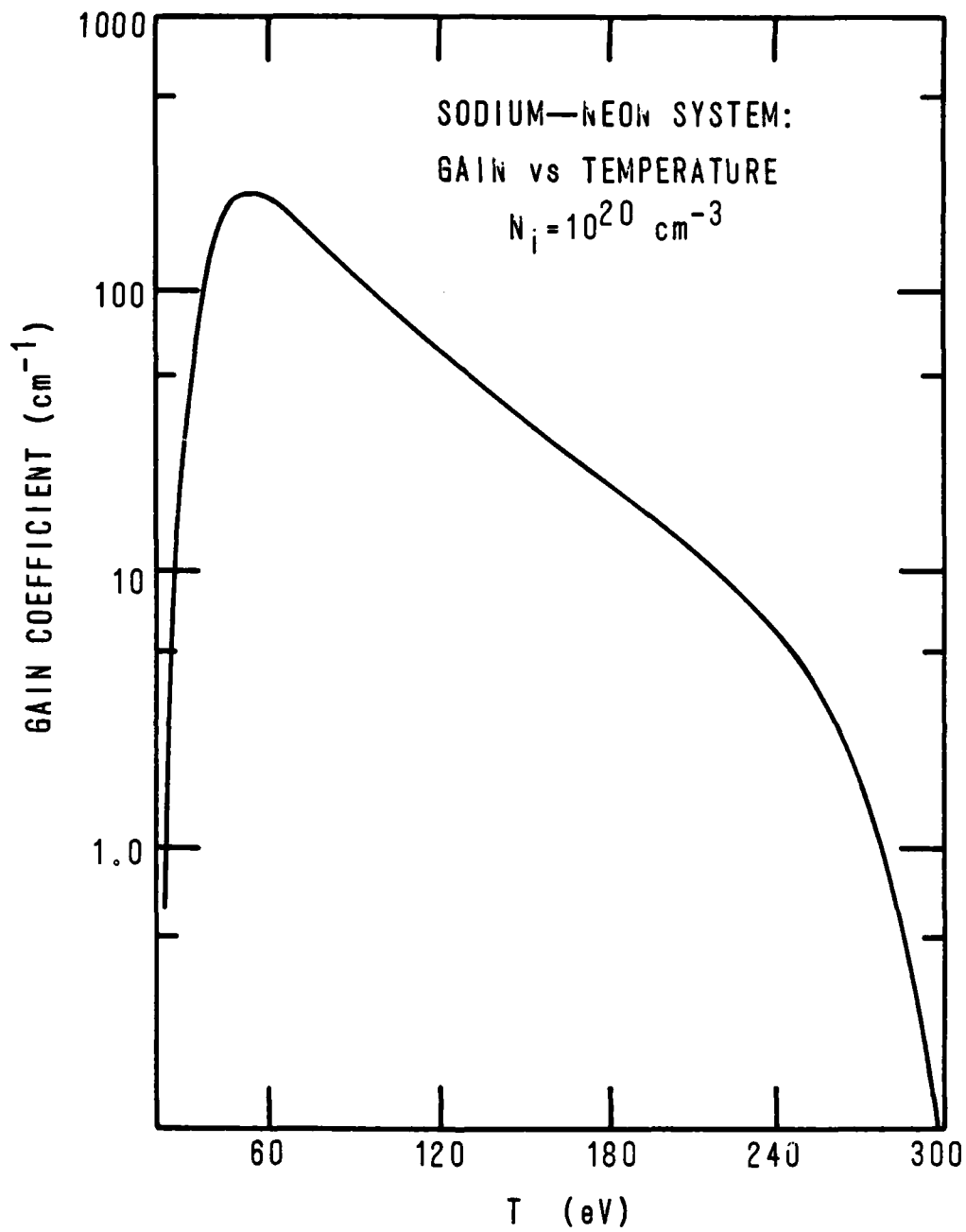


Fig. 5 — Line center gain coefficient in the Ne IX  $2p^1P-3d^1D$  line is plotted vs. Ne plasma temperature for a fixed Ne ion density of  $10^{20} \text{ cm}^{-3}$ .

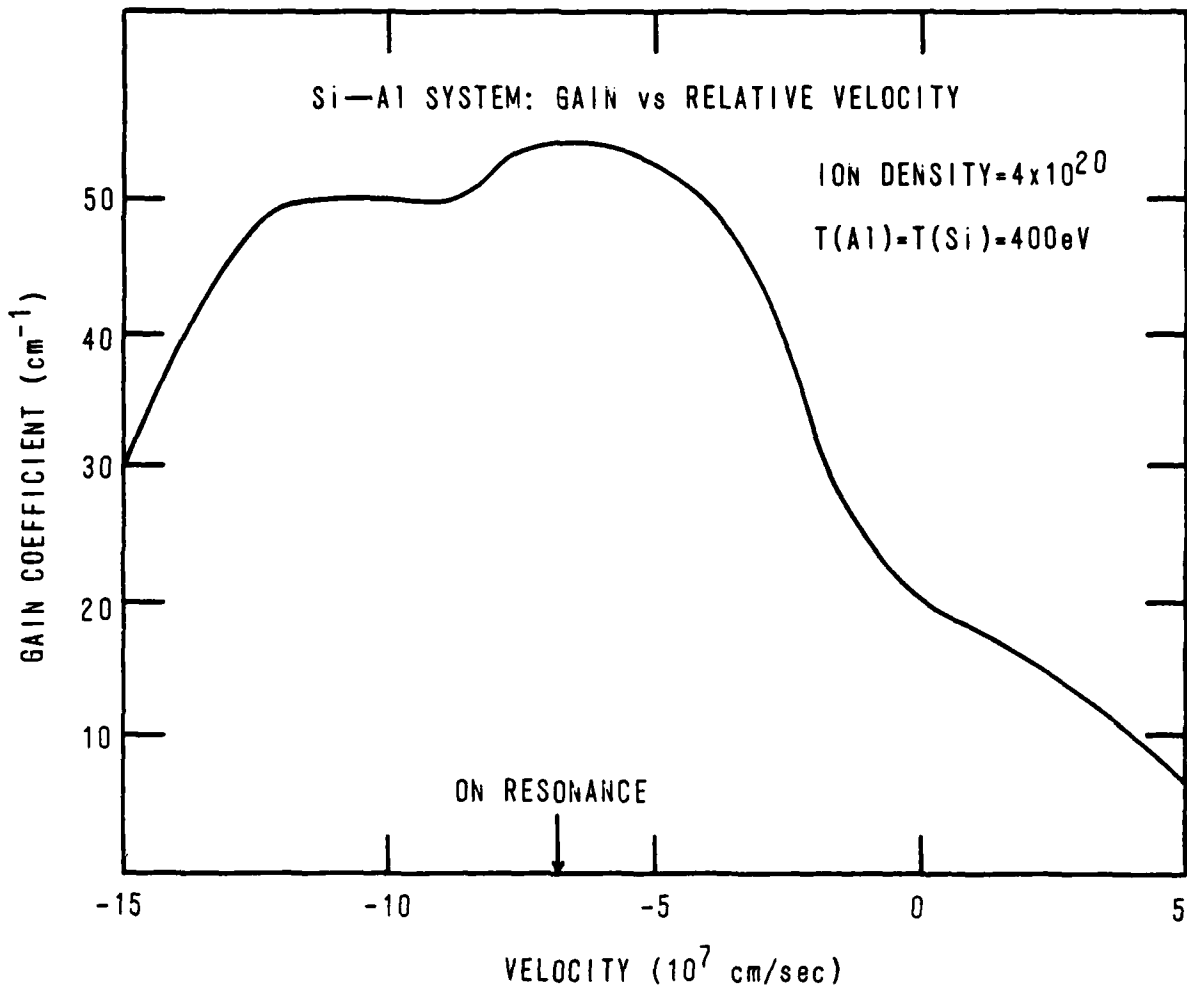


Fig. 6 — Line center gain coefficient in the Al XII  $2p^1P-3d^1D$  line is plotted vs. velocity of approach of the Si and Al plasmas. The Al ion density is  $4 \times 10^{20} \text{ cm}^{-3}$  and its temperature (the same as that of the pumping Si plasma) is assumed to be 400 eV.

cm sec<sup>-1</sup>. This is due to the fact that most of the pumping radiation is not normally incident on the pumped plasma and therefore a range of velocity shifts are sampled (due to the  $\cos \theta$  effect) at any one physical streaming velocity. At the perfectly matched streaming velocity of  $6.8 \times 10^7$ , gain is -3 times that of zero streaming velocity because the very highest pumping line intensities just outside the self reversed core are sampled to the greatest degree. Having the two components, Si and Al, approach each other is therefore helpful, but not essential to the scheme's basic viability.

#### IV. Further Remarks and Conclusions

We have determined through a series of detailed calculations the conditions under which significant gain at x-ray wavelengths, employing the Na/Ne and Si/Al plasmas for resonant photon pumping, should be attainable in the laboratory. Substantial gain at  $82 \text{ \AA}$  and  $44 \text{ \AA}$  for Na/Ne and Si/Al, respectively, is in principle achievable, as documented in Figs. 2-6. However, the task of setting up the correct plasma conditions is not trivial for a number of reasons. For optimum employment of both schemes, the temperature of the pumped plasma should be maintained well below that of the pumping plasma to avoid excessive ionization in the lasing medium. This could perhaps be accomplished by keeping the two components as physically separate as possible to reduce conductive temperature equilibration. Similarly, the pumping plasma might be heated first, and then the pumped medium activated through use of a delayed heating pulse or laser beam to assure that the pumped plasma passes through the optimal temperature range while being exposed to the intense pumping radiation. Also, in previously successful experiments<sup>14</sup>, stepped targets using metal plates as heat sinks have allowed experimenters to tune the plasma temperature downward at certain distances from the initial plasma formation surface. Perhaps similar techniques could be employed for the present schemes. Even though a lower pumped plasma temperature is essential for optimum steady state gain, substantial gain is still achievable for equal pumped and pumping plasma temperatures (Fig. 6).

In the case of the Na/Ne system, pumping radiation was generated in an actual pellet implosion experiment at Rochester for which the ion density of the pellet has been diagnosed as  $4.5 \times 10^{21} \text{ cm}^{-3}$ <sup>8</sup>, which is more than an order of magnitude greater than the neon ion density required for maximum gain. In short,

a very dense sodium plasma is desirable to obtain high pumping power, but a relatively tenuous neon medium is needed to prevent collisional processes from neutralizing the pumped inversion. Therefore, a configuration which is the reverse of a normal pellet suggests itself. One might compress a cylindrical glass rod (with a cylindrically focussed laser, perhaps) which has been heavily doped with sodium impurities. This rod would initially be encased in neon, which would form a more tenuous blowoff plasma. Or, alternatively two physically separate Na and Ne plasmas could be created with intensities and pulse widths tailored to produce optimum gain characteristics. This would certainly allow different densities to be produced in the separate components, and would minimize or eliminate conductive temperature equilibration. Since ionization of the pumped plasma by pumping radiation other than the resonance line did not present any serious difficulties in the Si/Al calculation, it would not be expected to present a problem in the Na/Ne case. However, this cannot be stated with complete confidence because, as mentioned above, only the Na resonance line radiation is assumed incident on the Ne in our calculations.

#### ACKNOWLEDGMENT

This work was supported in part by the Defense Nuclear Agency.

#### REFERENCES

1. A.V. Vinogradov, I.I. Sobelman, and E.A. Yukov, *Kvant. Electron. (Moscow)* 2, 105(1975) [*Sov. J. Quantum Electron.* 5, 59 (1975)].
2. B.A. Norton and N.J. Peacock, *J. Phys. B* 8, 989 (1975).
3. V.A. Bhagavatula, *J. Appl. Phys.* 47, 4535 (1976).
4. J.P. Apruzese, J. Davis, and K.G. Whitney, *J. Phys. B* 11, L643 (1978).
5. V.A. Bhagavatula, *Appl. Phys. Lett.* 33, 726 (1978).
6. V.A. Bhagavatula, *IEEE J. Quantum Electron.* 16, 603 (1980).
7. K.G. Whitney, J. Davis, and J.P. Apruzese, *Phys. Rev. A* 22, 2196 (1980).
8. J.P. Apruzese, P.C. Kepple, K.G. Whitney, J. Davis, and D. Duston, *Phys. Rev. A.*, in press.
9. H.R. Griem, M. Blaha, and P.C. Kepple, *Phys. Rev. A* 19, 2421 (1979).
10. B. Yaakobi, D. Steel, E. Thorsos, A. Hauer, and B. Perry, *Phys. Rev. Lett.* 39, 1526 (1977).
11. P. Burkhalter, J. Davis, J. Rauch, W. Clark, G. Dahlbacka, and R. Schneider, *J. Appl. Phys.* 50, 705 (1979).
12. K.G. Whitney, J. Davis, and J.P. Apruzese, "Some Effects of Radiation Trapping on Stimulated VUV Emission in Ar XIII", in Cooperative Effects in Matter and Radiation, edited by C.M. Bowden, D.W. Howgate, and H.R. Robl (Plenum, New York, 1977).
13. V.L. Jacobs, J. Davis, J.E. Rogerson, and M. Blaha, *Astrophys. J.* 230, 627 (1979); also unpublished calculations for Al.
14. V.A. Bhagavatula and B. Yaakobi, *Opt. Commun.* 24, 331 (1978).

DISTRIBUTION LIST

Commanding Officer  
Naval Intelligence Support Center  
4301 Suitland Road, Bldg. 5  
Washington, D.C. 20390  
ATTN: NISC-45

Commander  
Naval Weapons Center  
China Lake, California 93555  
ATTN: Code 233 (Tech. Lib.)

Office of the Chief of Naval Operations  
Washington, D.C. 20350  
ATTN: R. Blaise

Officer in Charge  
White Oak Laboratory  
Naval Surface Weapons Center  
Silver Spring, Maryland 20910  
ATTN: Code R40 (1 copy)  
ATTN: Code F31 (1 copy)

Space and Missile Systems Organization/IN  
Air Force Systems Command  
Post Office Box 92960  
Worldway Postal Center  
Los Angeles, California 90009  
ATTN: IND D. Muskin (Intelligence)

Space and Missile Systems Organization/MN  
Air Force Systems Command  
Norton AFB, California 92409  
ATTN: MNNH (Minuteman)

Space and Missile Systems Organization/SK  
Air Force Systems Command  
Post Office Box 92960  
Worldway Postal Center  
Los Angeles, California 90009  
ATTN: SKF P. Stadler (Space Comm. Systems)

AVCO Research and Systems Group  
201 Lowell Street  
Wilmington, Massachusetts 01887  
ATTN: Library A830

BDM Corporation  
7915 Jones Branch Drive  
McLean, Virginia 22101  
ATTN: Corporate Library

Boeing Company  
P.O. Box 3707  
Seattle, Washington 98124  
ATTN: Aerospace Library

Dikewood Industries, Inc.  
1009 Bradbury Drive, S.E.  
Albuquerque, New Mexico 87106  
ATTN: L. Davis

EG and G Washington Analytical Services Center, Inc.  
P. O. Box 10218  
Albuquerque, New Mexico 87114  
ATTN: Library

General Electric Company  
Space Division  
Valley Forge Space Center  
P.O. Box 8555  
Philadelphia, Pa. 19101  
ATTN: J. Peden

Institute for Defense Analyses  
400 Army-Navy Drive  
Arlington, VA 22202  
ATTN: Classified Library

IRT Corporation  
P.O. Box 81087  
San Diego, California 92138  
ATTN: R. Mertz

JAYCOR  
1401 Camino Del Mar  
Del Mar, California 92014  
ATTN: E. Wenaas

JAYCOR  
205 S. Whiting Street, Suite 500  
Alexandria, Virginia 22304  
ATTN: R. Sullivan

Lawrence Livermore National Laboratory  
University of California  
P.O. Box 808  
Livermore, California 94550  
ATTN: DOC CDN for L-545 J. Nickolls  
ATTN: DOC CDN for L-153  
ATTN: DOC CDN for L-47 L. Wouters  
ATTN: DOC CDN for Technical Infor. Dept. Lib.

Lockheed Missiles and Space Co., Inc.  
3251 Hanover Street  
Palo Alto, California 94304  
ATTN: L. Chase

Maxwell Laboratory, Inc.  
9244 Balboa Avenue  
San Diego, California 92123  
ATTN: A. Kolb  
ATTN: W. Clark  
ATTN: J. Pearlman

McDonnell Douglas Corp.  
5301 Bolsa Avenue  
Huntington Beach, California 92645  
ATTN: S. Schneider

Mission Research Corp.  
P.O. Drawer 719  
Santa Barbara, California 93102  
ATTN: C. Longmire  
ATTN: W. Hart

Mission Research Corp.-San Diego  
P.O. Box 1209  
La Jolla, California 92038  
ATTN: Victor J. Van Lint

Northrop Corporation  
Northrop Research and Technology Center  
1 Research Park  
Palos Verdes Peninsula, California 90274  
ATTN: Library

Physics International Company  
2700 Merced Street  
San Leandro, California 94577  
ATTN: C. Stallings  
ATTN: E. Goldman

R and D Associates  
P.O. Box 9695  
Marina Del Ray, California 90291  
ATTN: W. Graham, Jr.  
ATTN: P. Haas

Sandia National Laboratories  
P.O. Box 5800  
Albuquerque, New Mexico 87115  
ATTN: DOC CON For G. Yonas  
ATTN: DOC CON For 3141

Science Applications, Inc.  
P.O. Box 2351  
La Jolla, California 92038  
ATTN: J. Beyster

Spire Corporation  
P.O. Box D  
Bedford, Massachusetts 01730  
ATTN: R. Little

SRI International  
333 Ravenswood Avenue  
Menlo Park, California 94025  
ATTN: S. Dairiki

Systems, Science and Software, Inc.  
P.O. Box 1620  
La Jolla, California 92038  
ATTN: A. Wilson

TRW Defense and Space Systems Group  
One Space Park  
Redondo Beach, California 90278  
ATTN: Technical Information Center

Vought Corporation  
Michigan Division  
38111 Van Dyke Road  
Sterling Heights, Maine 48077  
ATTN: Technical Information Center  
(Formerly LTV Aerospace Corp.)

Naval Research Laboratory  
Plasma Radiation Group  
Washington, D.C. 20375

Code 4707	-	
Code 4700	- 26 Copies	(unclassified only) (1 copy if classified)
Code 6534	-	
Code 4730	- S. Bodner	